

Dispersal of Mass and Circulation Following Shock-sphere and Shock-cylinder Interactions:

Effects arising from shock cavity collapse, vortex bilayers, density-gradient intensification and vortex projectiles



G. Peng, S. Gupta, S. Zhang and N.J. Zabusky

**Laboratory for Visiometrics and Modeling
Department of Mechanical and Aerospace Engineering
Rutgers University**

Motivations

- Mass and vorticity dispersal in strong- shock-sphere and shock-cylinder interactions
- Secondary structures: vortex bilayers and vortex projectiles (VPs)
- Shock cavity implosion morphology and pressure enhancement
- Secondary baroclinic vorticity generation and instability: Density gradient intensification.

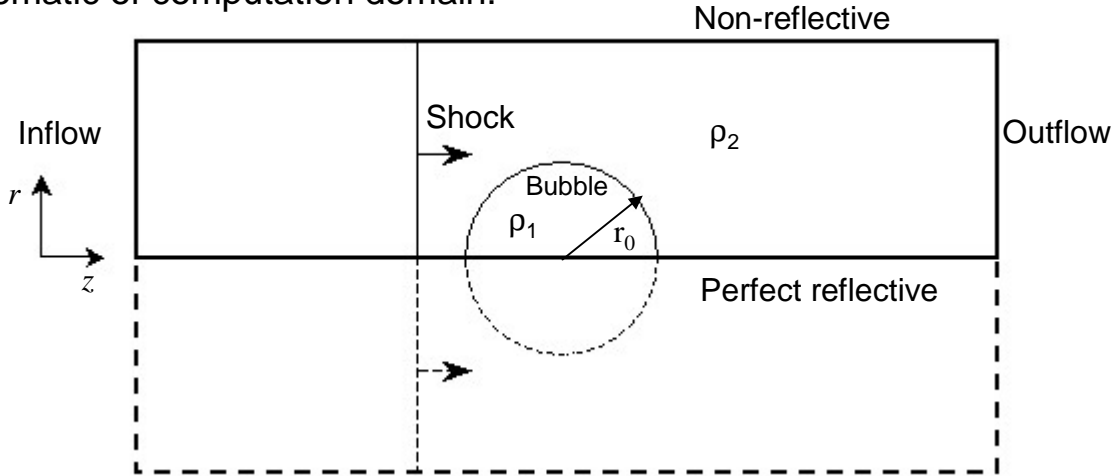
Brief Review:
Shock-sphere and shock-cylinder

1. JF Haas and B. Sturtevant, 1987, J. Fluid Mech.
2. J.M. Picone and J.P. Boris, 1989, J. Fluid Mech.
3. JW Jacobs, 1993, Phys. Fluids
4. R Samtaney and NJ Zabusky, 1993, J. Fluid Mech.
5. R Klein, CF Mckee and P. Colella, 1994, Astrophys. J.
6. JJ Quirk and S Karni, 1996, J. Fluid Mech.
7. NJ Zabusky and SM Zeng, 1998, J. Fluid Mech.

Part I: Shock -sphere Interaction

2D Axisymmetric Compressible Euler Simulation with PPM

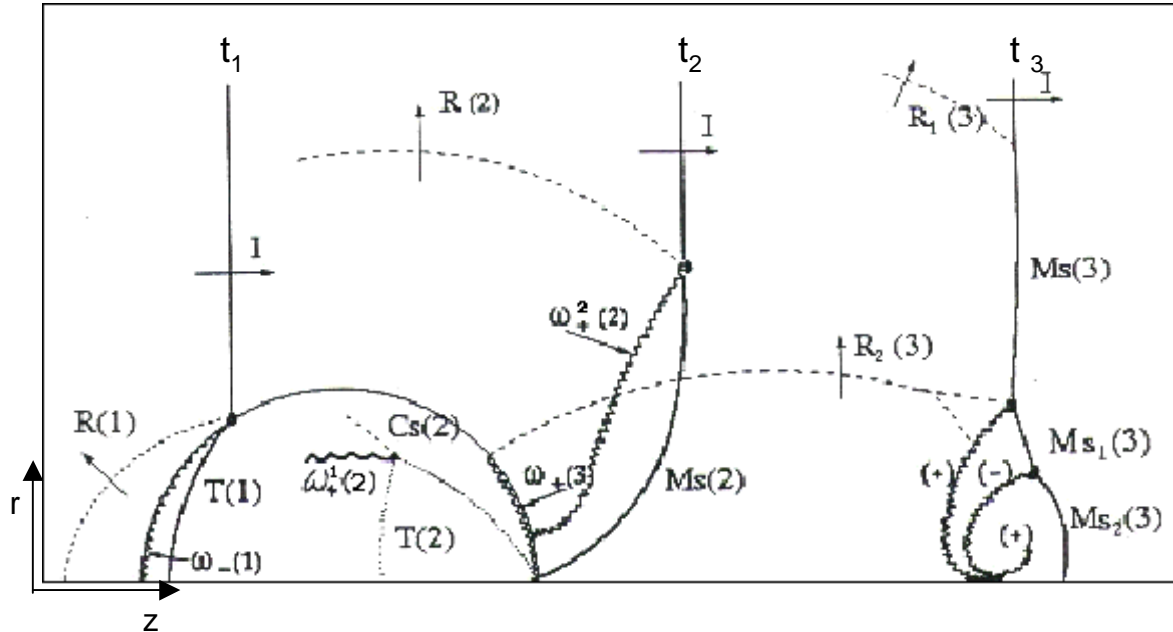
➤ Schematic of computation domain:



➤ Parameter domain:

M (shock)	$\rho_1 / \rho_2 = \eta$	resolution	r_0
2.5, 5.0, 10.0	10.0	1606(r) × 246(z)	110 (zones)

Abstraction of Structures : Bubble; Shocks & Shear Layers at Early and Intermediate Times*



t_1 : $\omega_-(1)$ is the primary vorticity deposition layer (Samtaney and Zabusky 1994), R(1) reflected shock wave, T(1) transmitted shock wave, I represents the incident shock

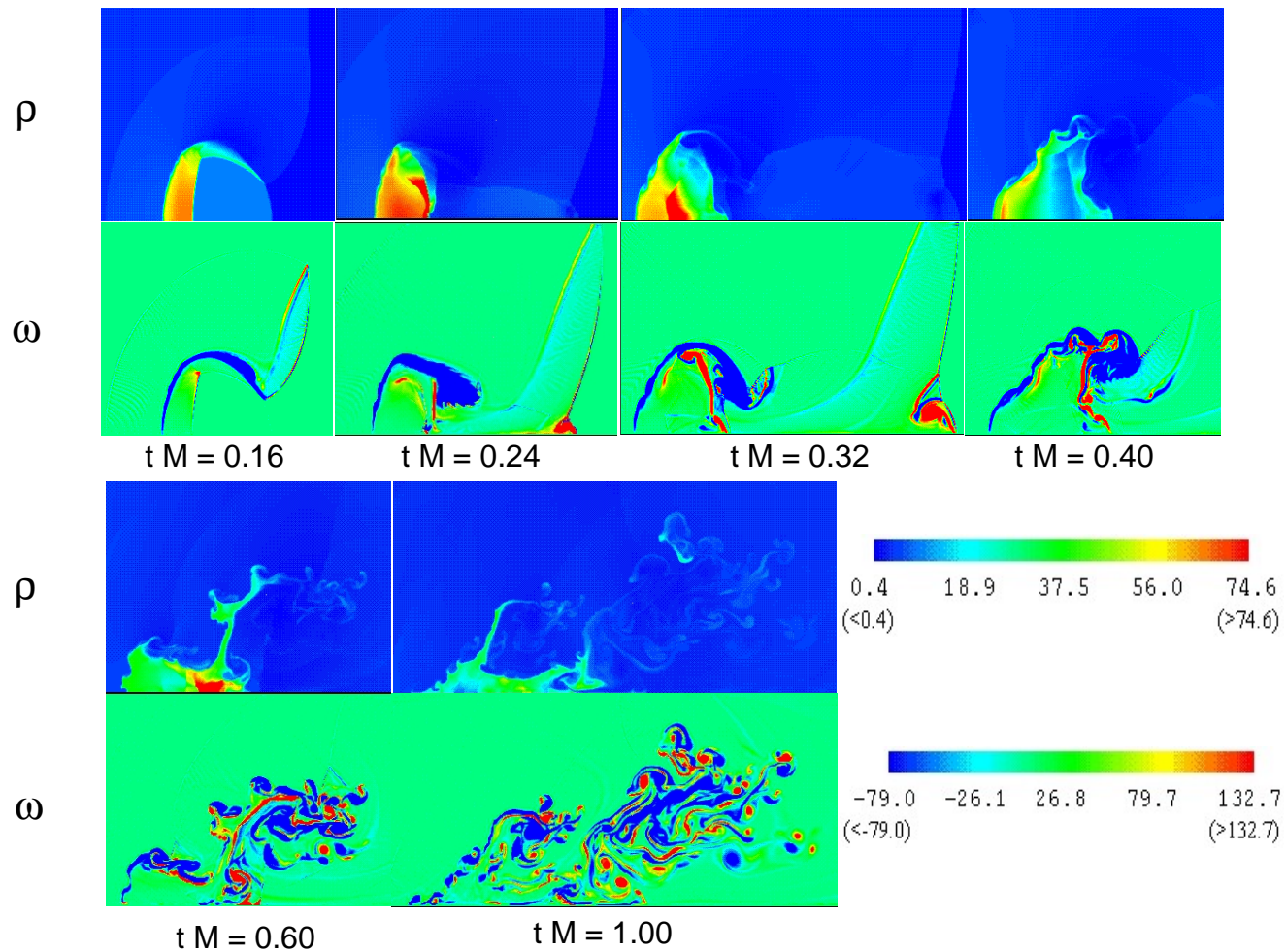
t_2 : $\omega_+(2)$ is a shear layer generated at the high curvature of transmitted shock T(2). R(2) is a reflected shock wave. Ms(2) is the Mach stem, and $\omega_+(2)$ is the shear layer produced at the triple point of Mach shock reflection. Transmitted shock T(2) forms a shock cavity that will collapse and re-expand.

t_3 : $\omega_+(3)$ is secondary generated positive shear layer due to a Mach reflected shock R₂(3); double Mach reflection is typified by Mach stems Ms(3), Ms₁(3) and Ms₂(3) together with complex shear layers and vortex ring.

(*The abstraction is dependent on Mach number)

Mass & Vorticity Evolution and Dispersal, Vortex Projectile Formation I

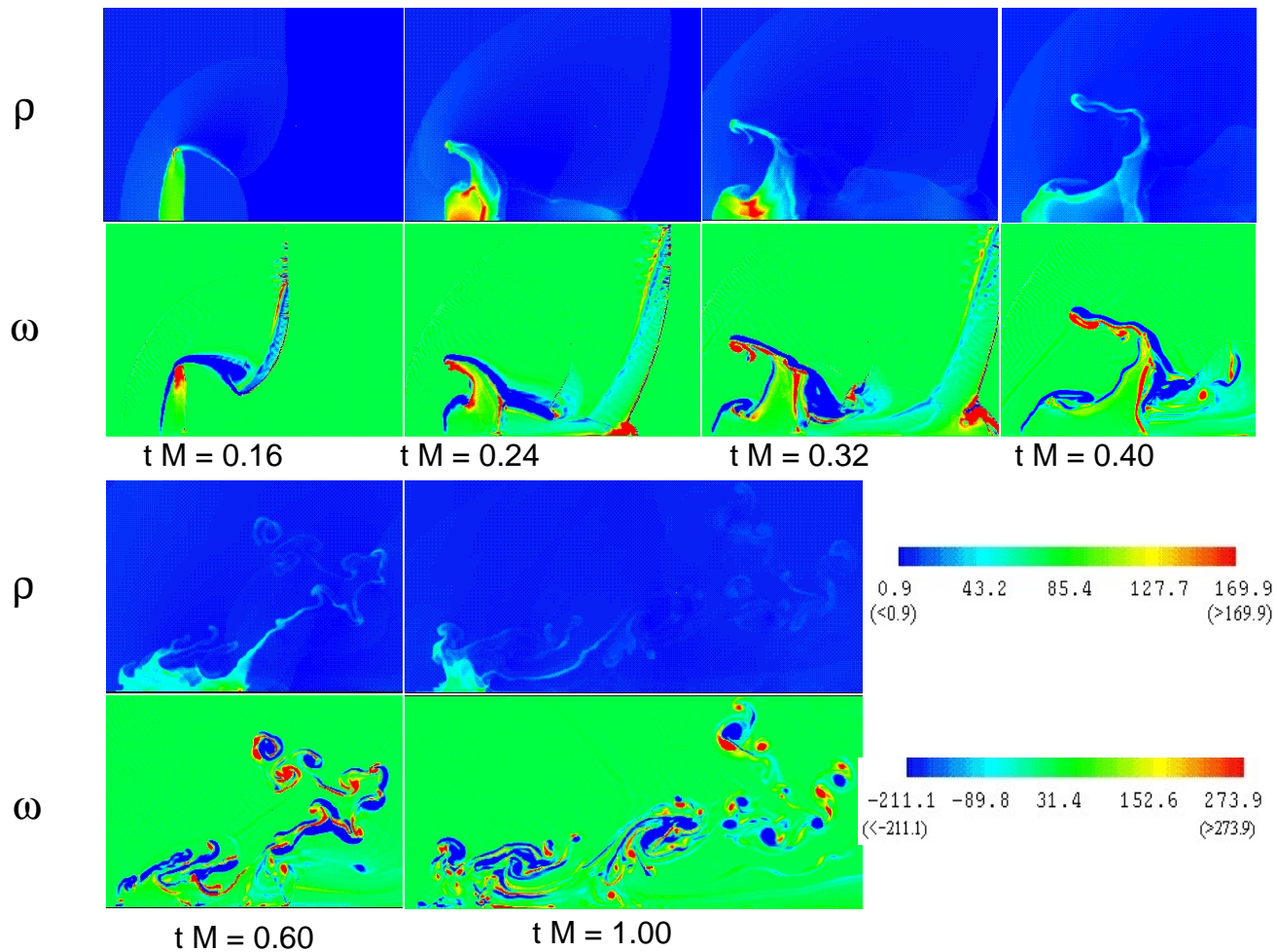
➤ Results for $M = 2.5$:



Vorticity (upper) and density (below) at normalized time

Mass & Vorticity Evolution and Dispersal, Vortex Projectile Formation II

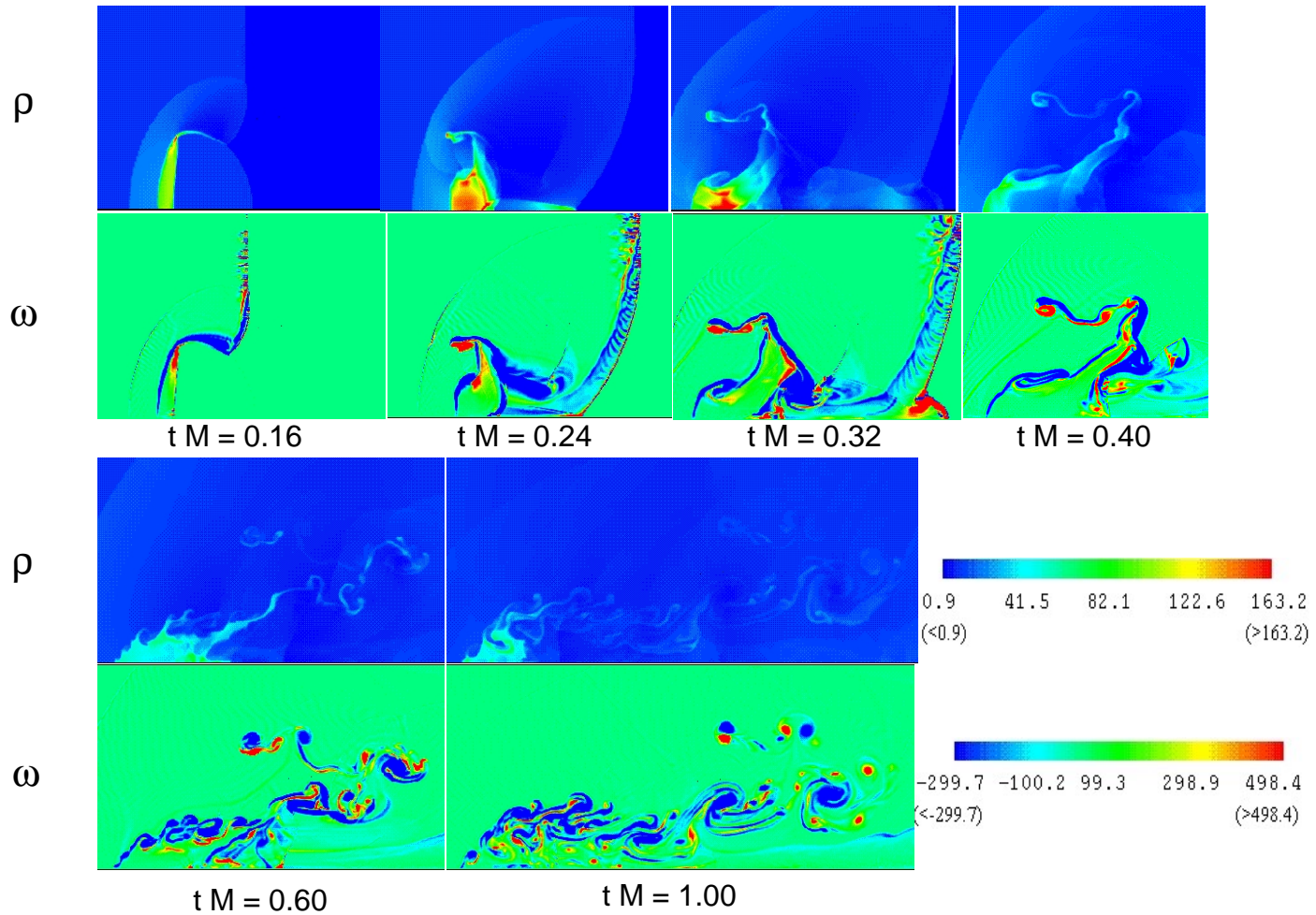
➤ Results for $M = 5.0$:



Vorticity (upper) and density (below) at normalized time

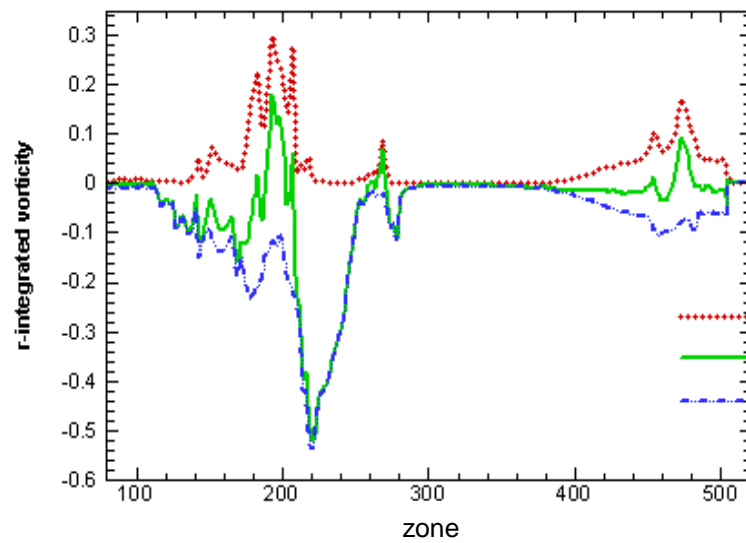
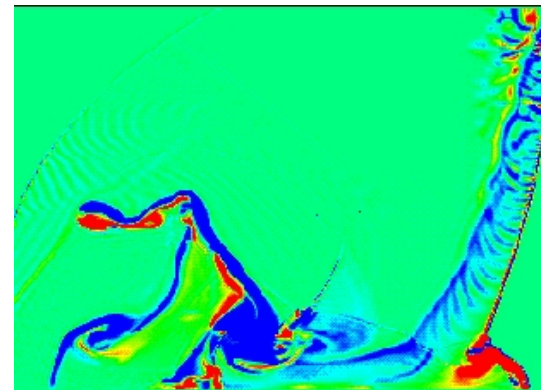
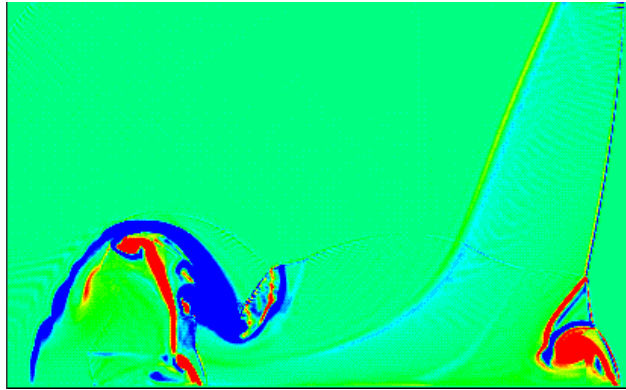
Mass & Vorticity Evolution and Dispersal, Vortex Projectile Formation III

➤ Results for $M = 10.0$:

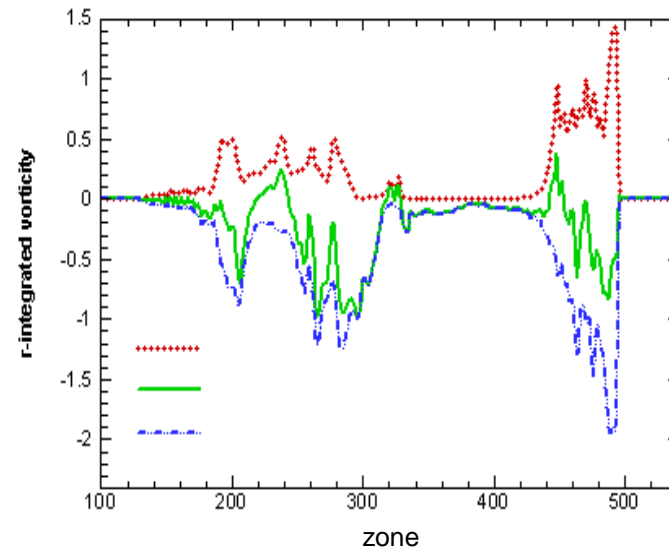


Vorticity (upper) and density (below) at normalized time

Y-integrated Vorticity Quantifies: Vortex bilayer and double mach reflection

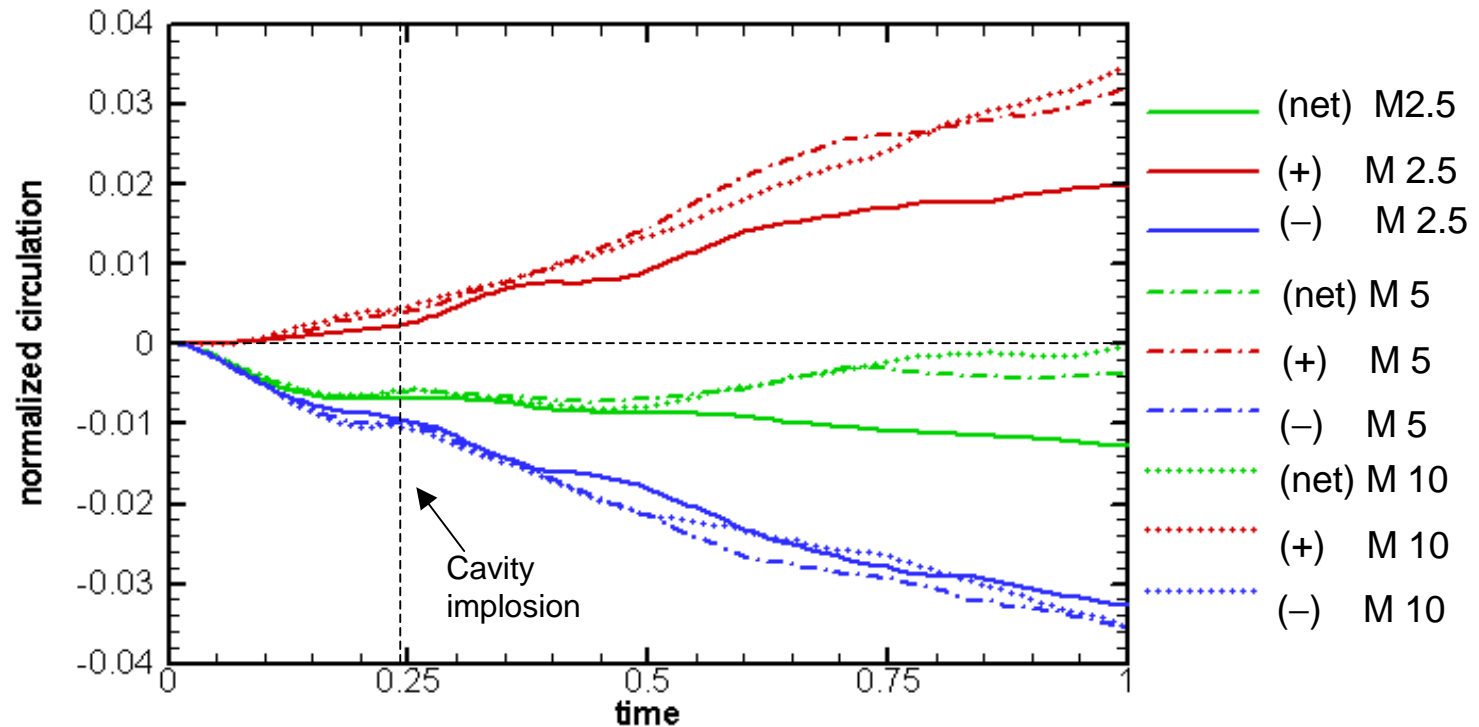


$M = 2.5$, $tM = 0.32$



$M = 10$, $tM = 0.32$

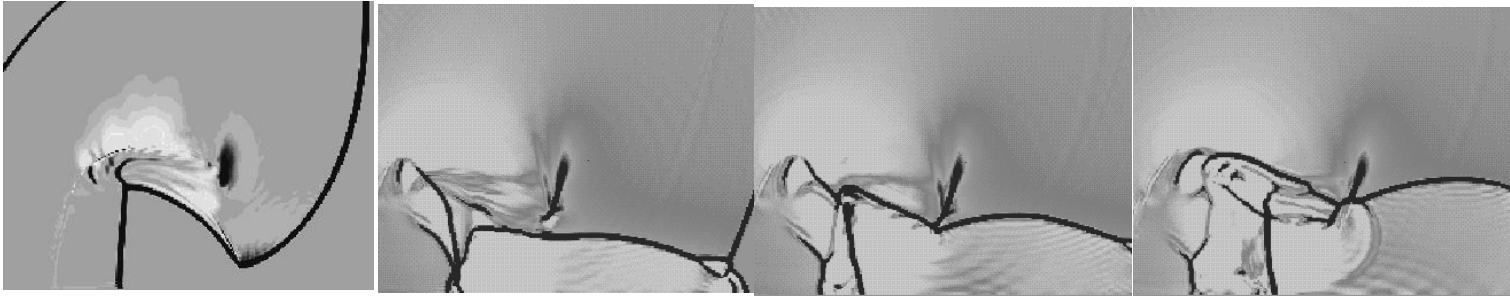
Global Circulation and Scaling



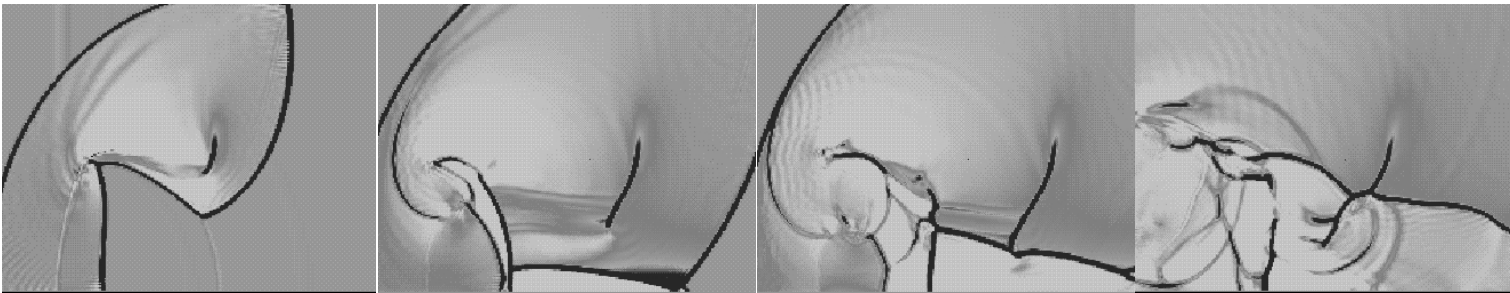
Circulation and normalization & scaling for different Mach numbers. $\Gamma \propto (M-1)(1+M^{-1}+2M^{-2})$ (Samtaney and Zabusky 1994) for circulation deposited on the interface. Secondary vorticity generation and double Mach reflection contributes to the circulation increase.

Shock-sphere Cavity: Implosion morphology

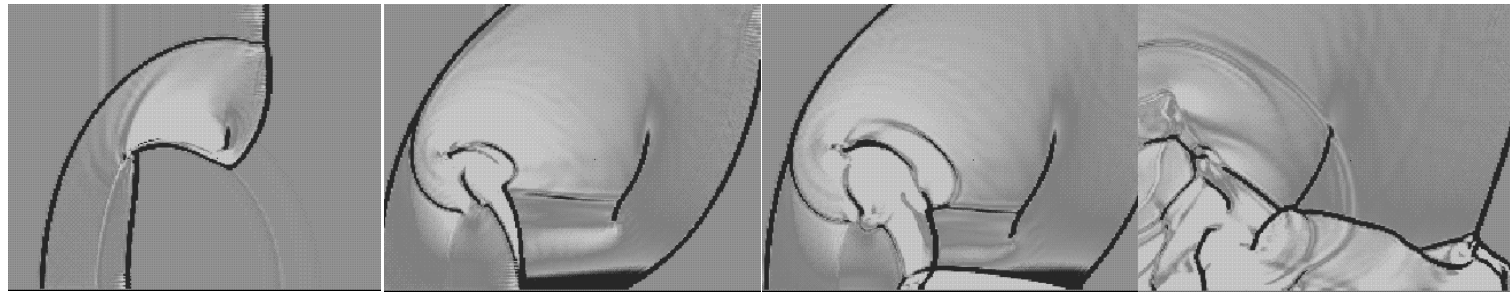
M = 2.5:
tM = 0.18, 0.24
, 0.26 , 0.29



M = 5.0:
tM = 0.16, 0.23
, 0.26, 32

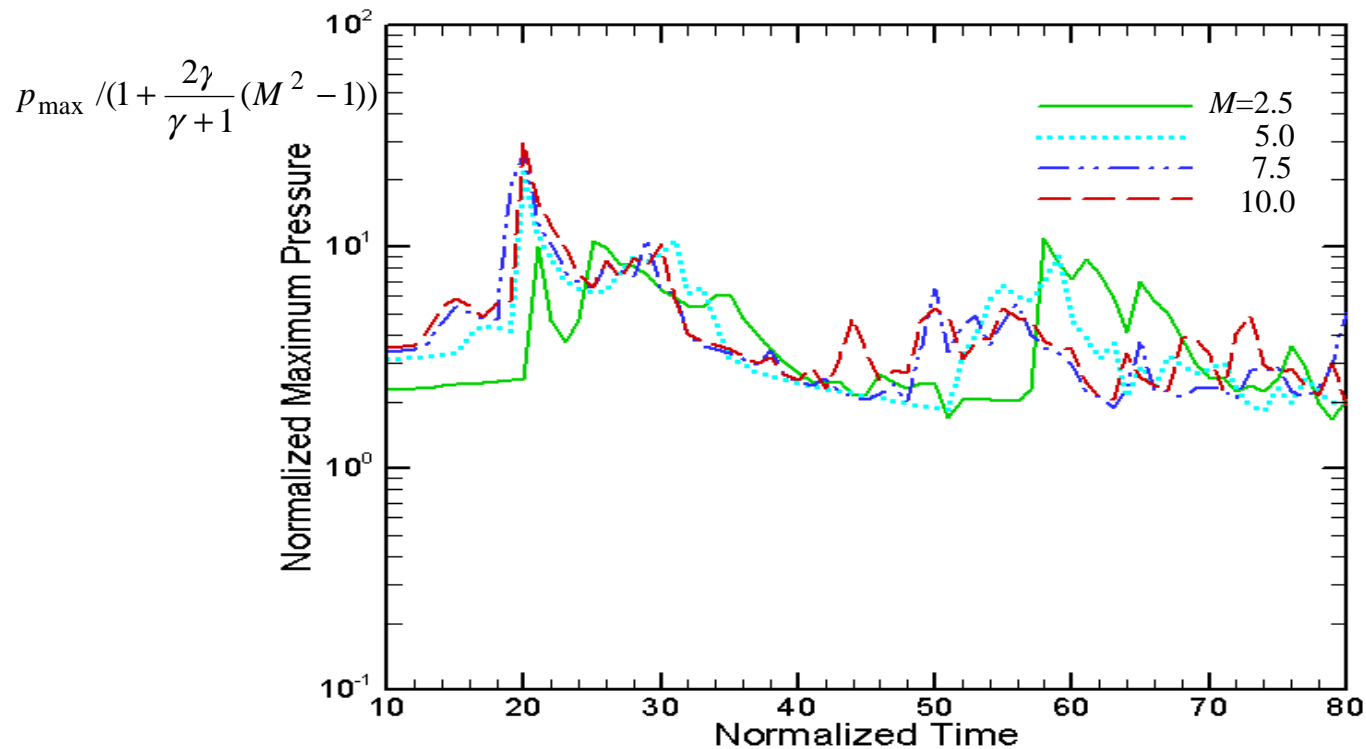


M = 10:
tM = 0.13, 0.22
, 0.24, 32



Divergence of velocity shows shock patterns, especially transmitted shock cavity implosion morphologies and double mach reflections. White represents expansion region.

Scaling Pressure Enhancement for Shock Cavity Collapse:



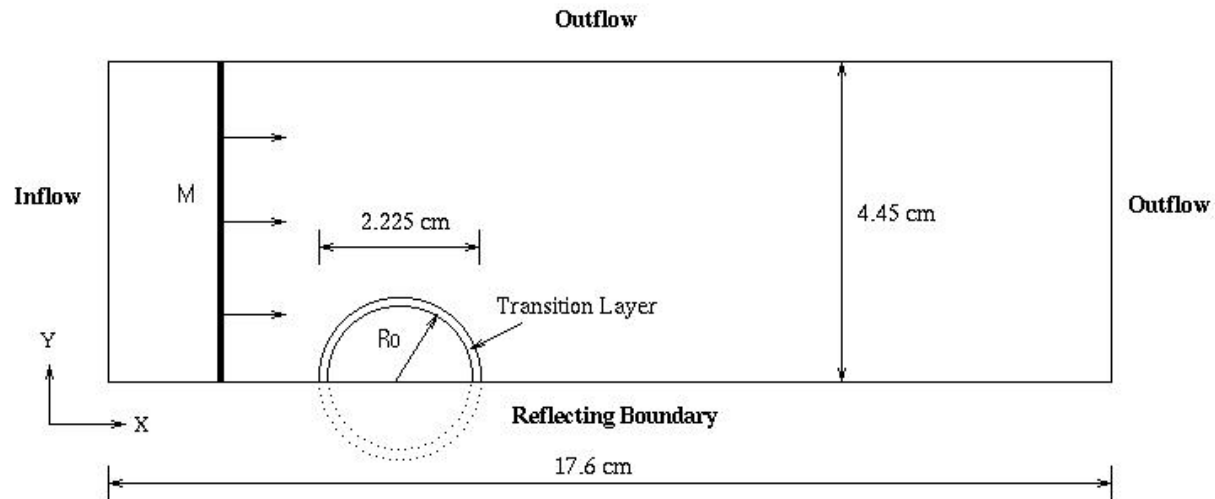
Scaling of maximum pressure ($M=2.5$ to 10 , $\eta=10$, $\gamma=1.209$). One dimensional pressure jump condition serves as a satisfactory scaling of pressure enhancement, especially at high Mach number since shock cavity implosion approaches one dimension collision of transmitted shocks. Time is normalized by the duration for the transmitted 1D shock to cross a bubble diameter.

Part II: Shock Cylinder Interaction

2D Cartesian Compressible Euler PPM Simulations

with finite interfacial transition layer

➤ Schematic of Computational Domain



Note: R_0 is $1/4^{\text{th}}$ the size of y-domain in all calculations. Figure not to the scale.

➤ Parameter domain

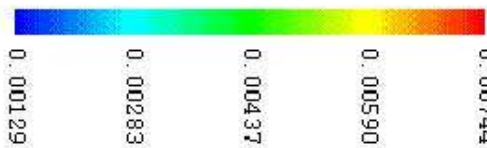
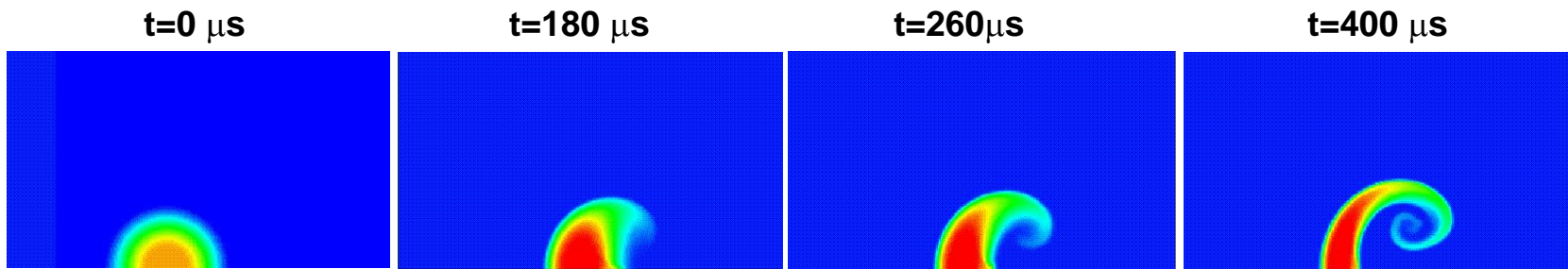
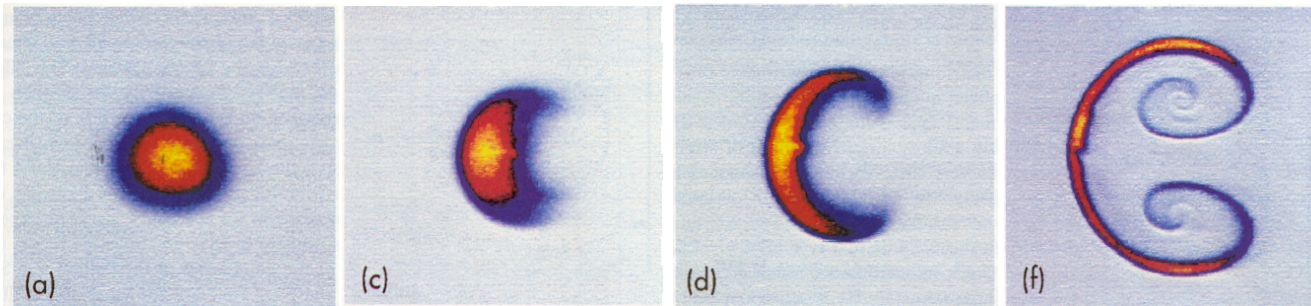
Mach No. (M)	Density Ratio(η)	Resolution
1.095,1.2	5.0	400*100,800*200,1200*300

➤ Numerical Method

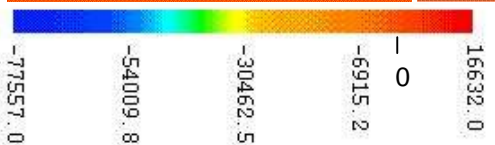
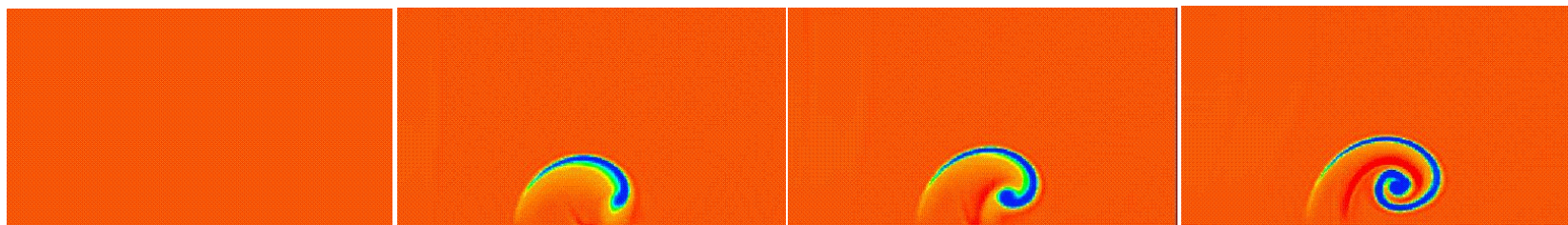
Compressible Euler Equations: Piecewise Parabolic Method

Mass and Circulation Evolution

Transition Layer with **Gaussian** Distribution: Comparison with Jacob's 1993 Experiment



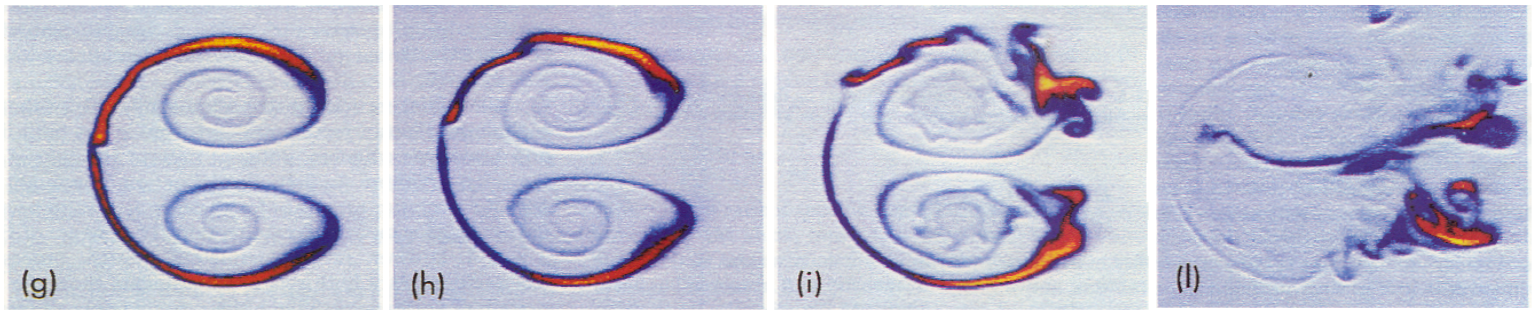
Density



Vorticity

(Mach 1.095, $\eta=5.0$, 800×200)

Mass and Circulation Evolution (Cont.)

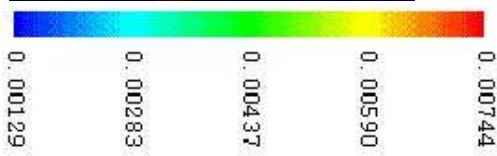
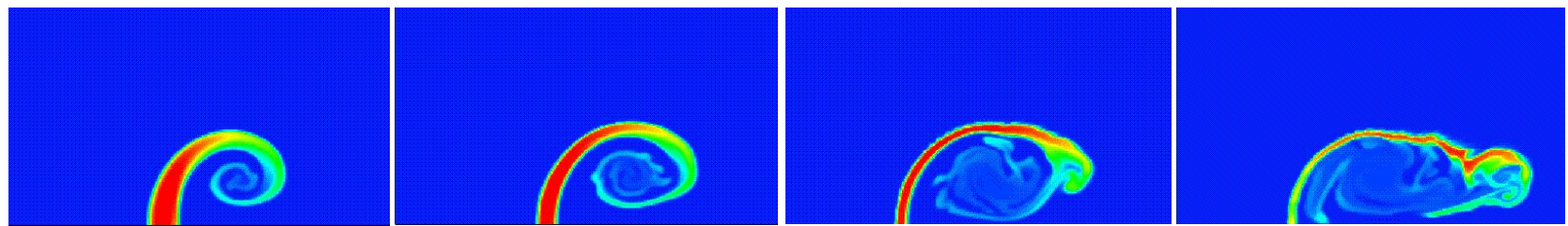


t=480 μ s

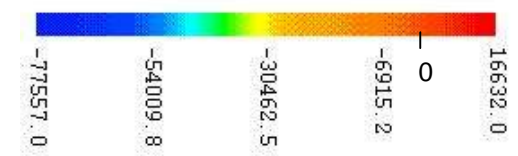
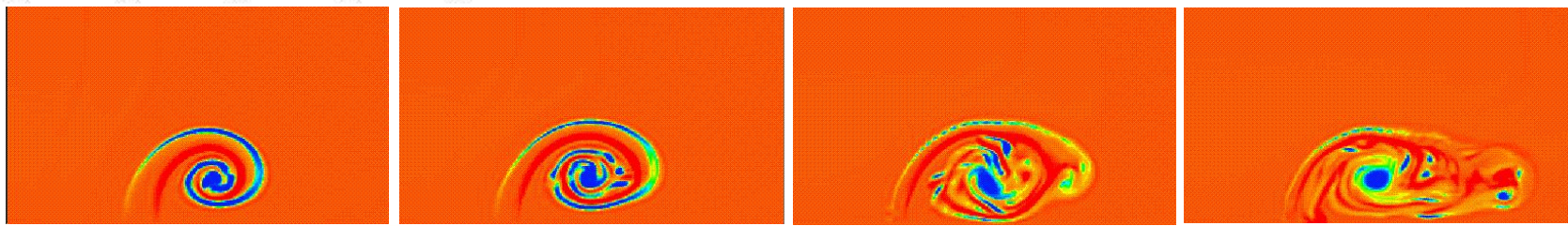
t=680 μ s

t=960 μ s

t=1340 μ s



Density

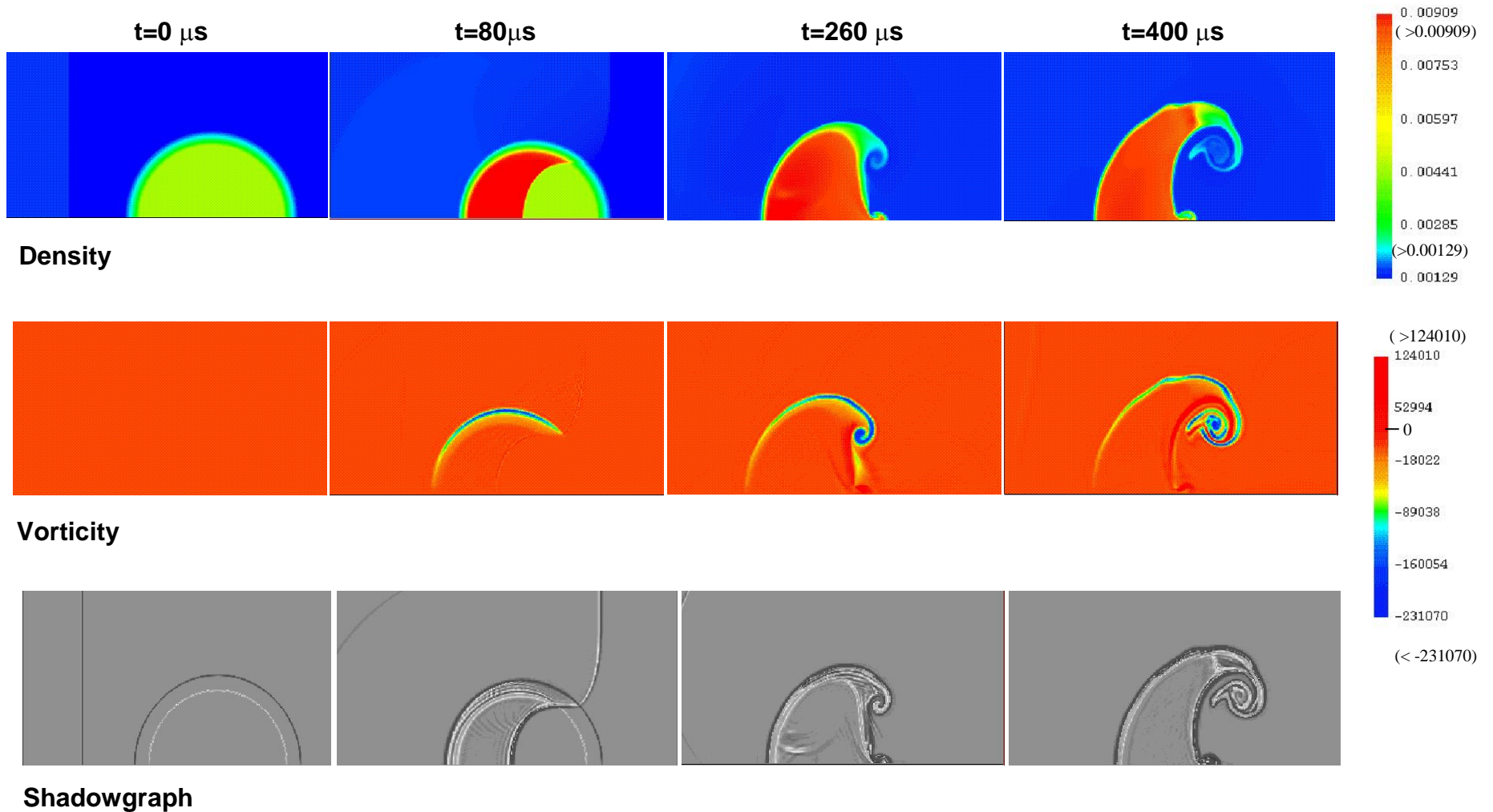


Vorticity

(Mach 1.095, $\eta=5.0$, 800*200)

Mass and Circulation Evolution

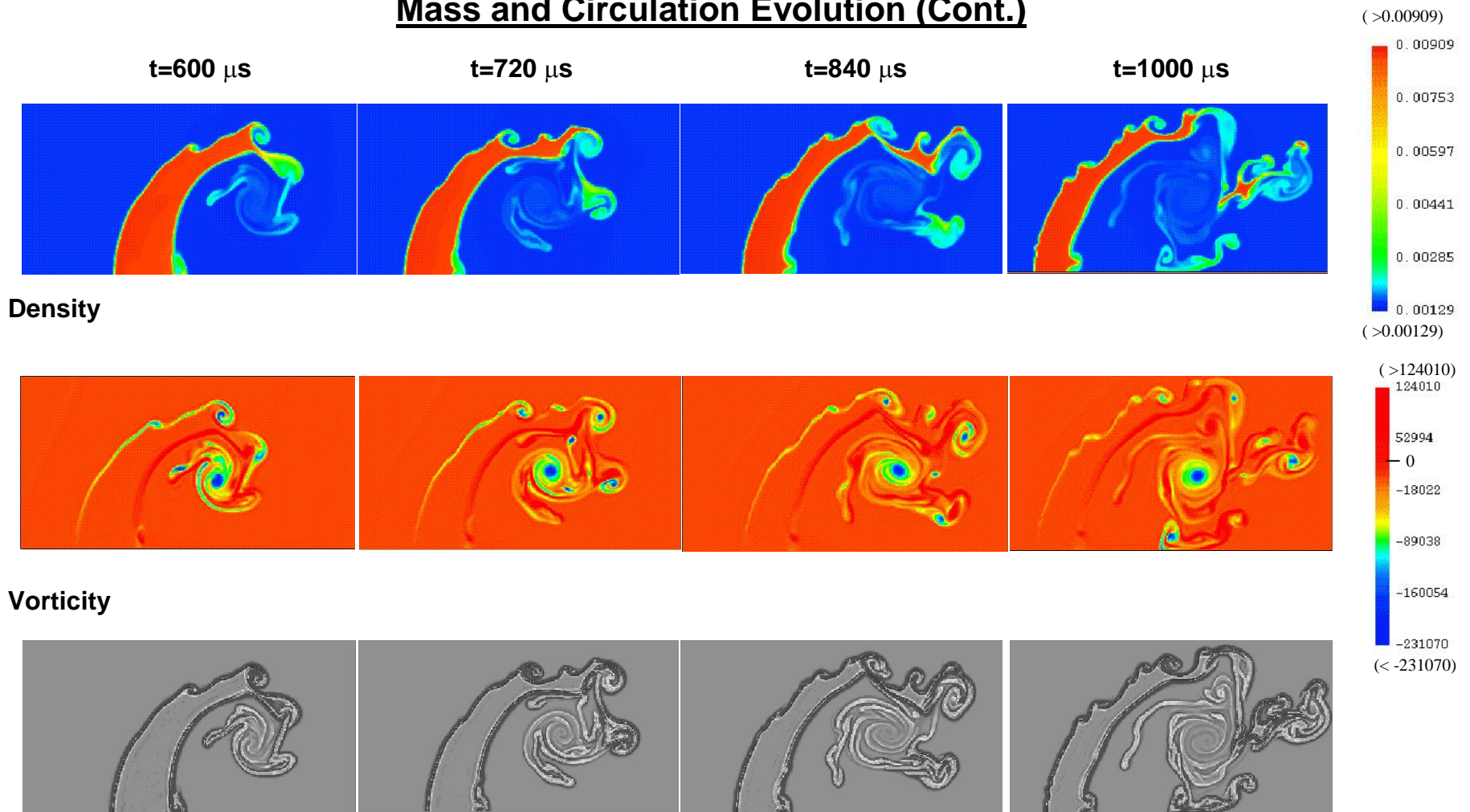
Transition Layer with a linear distribution



Early time evolution of mass and circulation using a linear transition layer between air and SF6 bubble.
Secondary roll-ups appear early in this configuration.

(Mach 1.2, $\eta=5.0$, 1200×300)

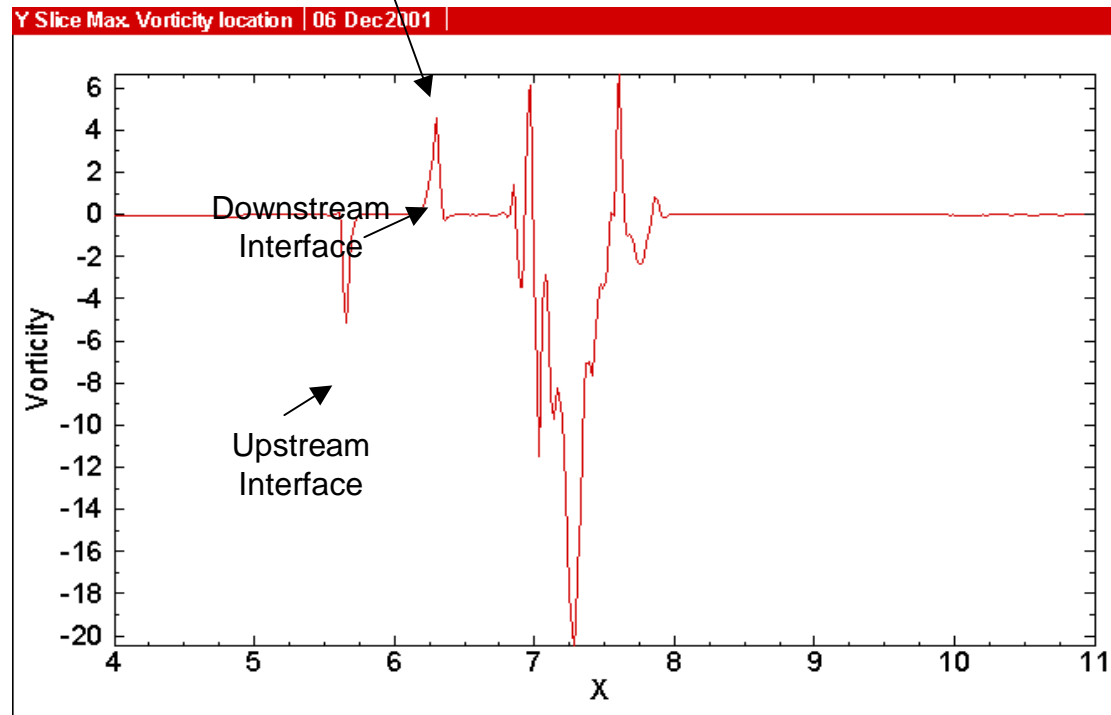
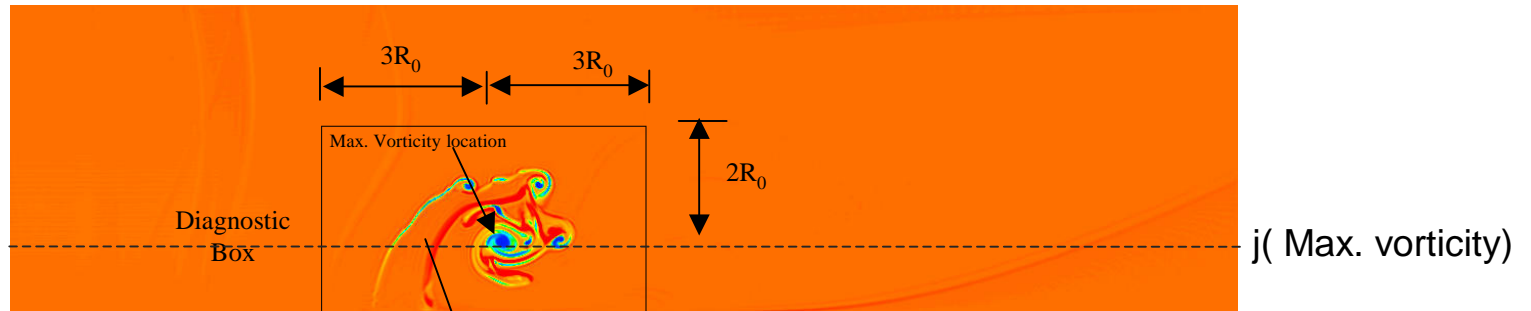
Mass and Circulation Evolution (Cont.)



Late time evolution of mass and circulation using a linear transition layer between air and SF6 bubble.
Vortex projectile formation and evolution at late time.

(Mach 1.2, $\eta=5.0$, 1200*300)

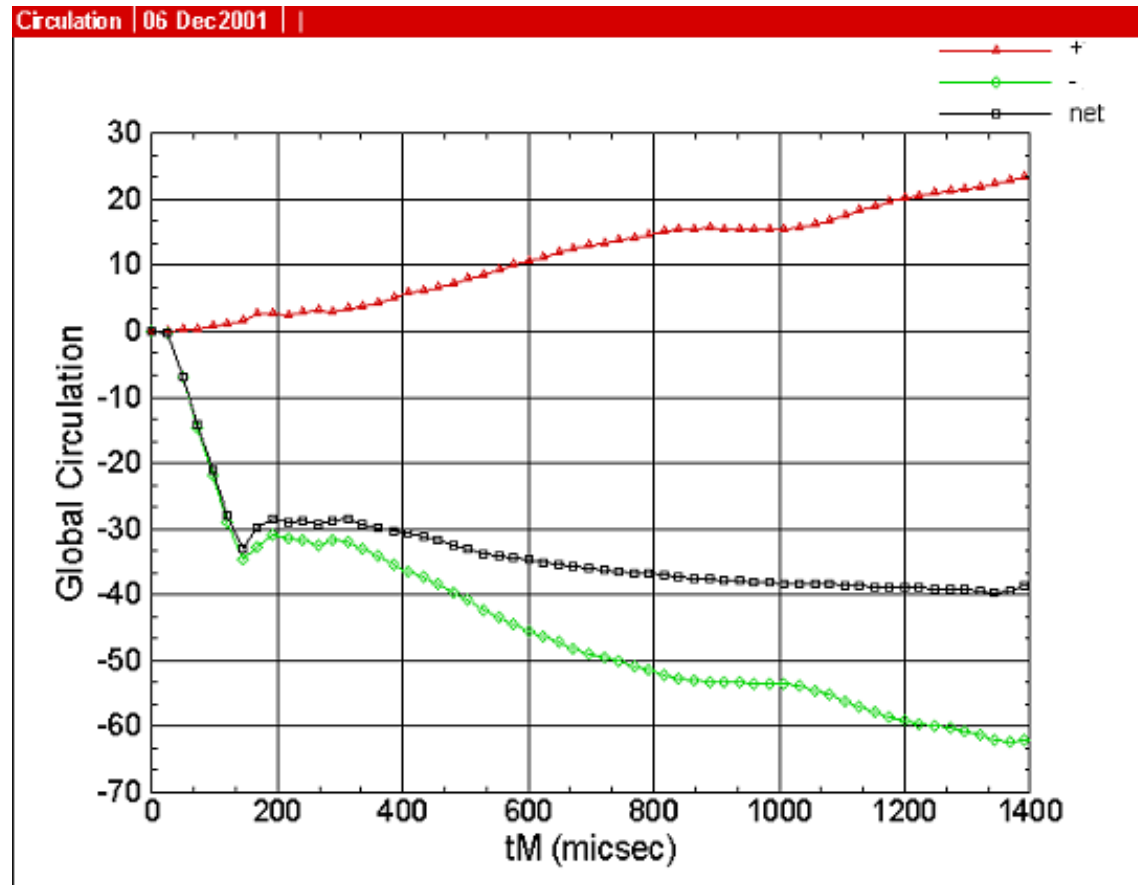
Vorticity Profile along a slice through vortex core at $t = 680\mu\text{s}$



Vorticity along a **y-slice** at location of maximum vorticity in the **diagnostic box** at $t = 680\mu\text{s}$. The peak correspond to the dominant vortex driving the flow after shock passage.

(Mach 1.2, $\eta=5.0$, 1200×300)

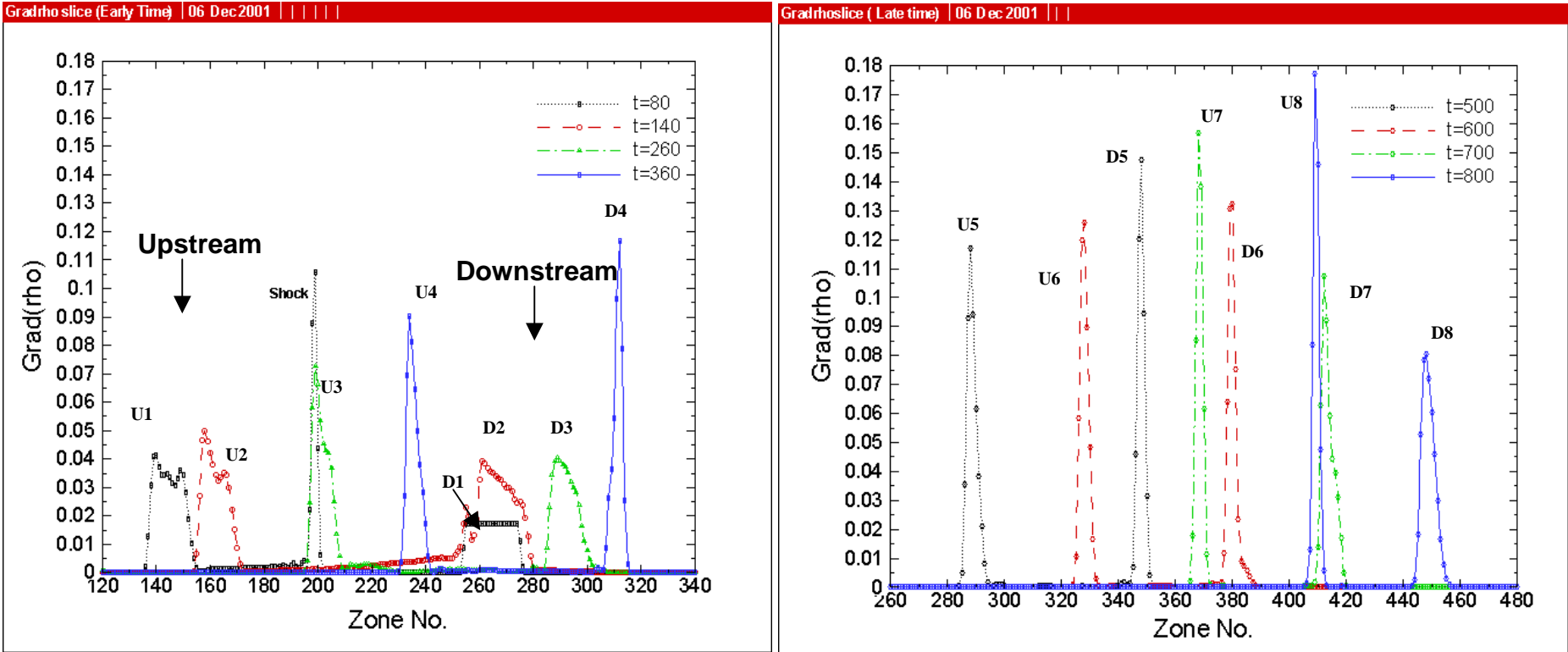
Global Circulation



Global circulation calculated in the diagnostic box. Increase in net circulation after primary vorticity deposition by shock passage due to secondary baroclinic effects.

(Mach 1.2, $\eta=5.0$, 1200×300)

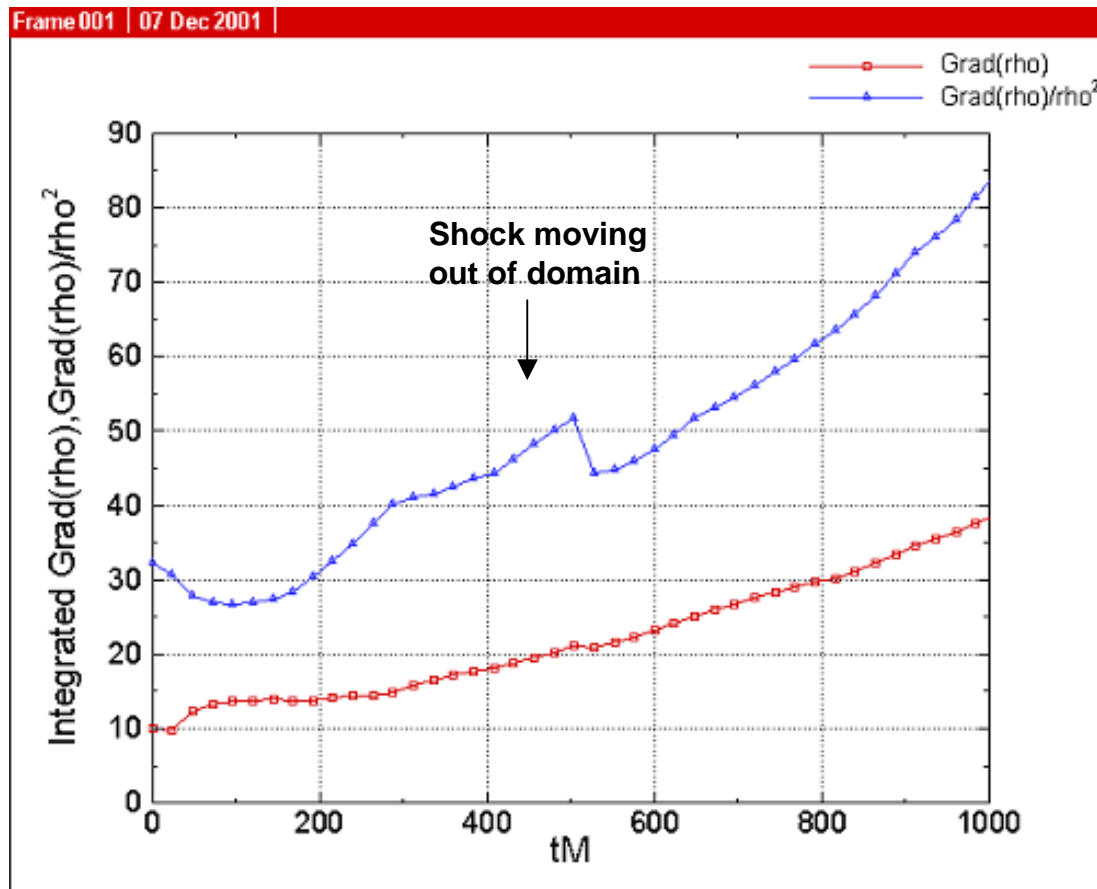
Density Gradient Intensification



Gradient of density $\nabla \rho$ along a slice at $j=25$. Same color peaks in each graph show upstream and downstream interface along this slice for various times showing the intensification of gradient of density.

(Mach 1.2, $\eta=5.0$, 1200×300)

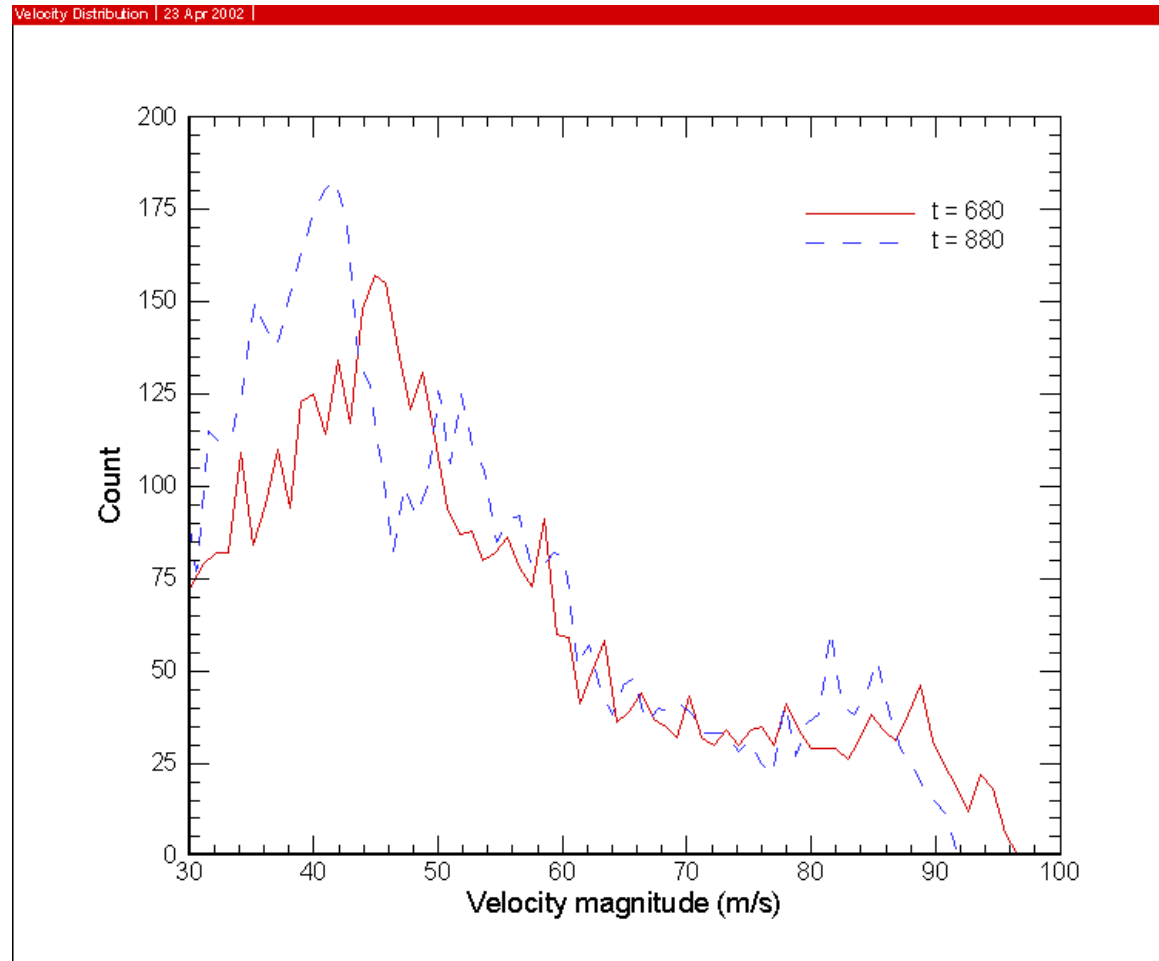
Density Gradient Intensification (Cont.)



Integrated $\nabla\rho$ and $\nabla\rho / \rho^2$ in the whole domain emphasizing the density gradient intensification.

(Mach 1.2, $\eta=5.0$, 1200*300)

Velocity Distribution



Velocity distribution in the diagnostic box at intermediate and late times showing a peak followed by large tail at the higher velocities. Velocities plotted are in a frame moving with a velocity upstream of the cylinder at the axis after passage of primary shock and reflected shock.

(Mach 1.2, $\eta=5.0$, 1200*300)

Conclusions

Part I: Shock Sphere($2.5 \leq M \leq 10$)

1. Observe intermediate time single vortex bilayer(VBL) for low Mach number and two VBLs for higher Mach number that evolves into a Vortex Projectiles (VPs).
2. Dominant contribution of VBLs to mass transport.
3. Circulation(+/-) growth stronger after cavity implosion.
4. Shock cavity implosion pressure enhancement $\propto 1 + \frac{2\gamma}{\gamma+1}(M^2 - 1)$

Part II: Shock Cylinder (M =1.095 & 1.2)

1. Primary and secondary structures agree with Jacob's Experiment ('93).
2. Initial finite Gaussian transition layer on gas cylinder motivated by experimental "setup" time
 - Initial Condition Parameterization: Interfacial gradient and core size.
3. **Opposite signed (+)** circulation evolves on downstream interface and is responsible for bubble elongation.
 - Secondary Baroclinic (+ / -) circulations ($\Delta\Gamma_- \approx 100\%$) result from interfacial density-gradient enhancement.
 - Velocity distribution in diagnostic box.